J. Chosun Natural Sci.
Vol. 10, No. 3 (2017) pp. 141 – 147
https://doi.org/10.13160/ricns.2017.10.3.141

Hologram Quantitative Structure-Activity Relationships Study of N-Phenyl-N'-{4-(4-quinolyloxy)phenyl} Urea Derivatives as VEGFR-2 Tyrosine Kinase Inhibitors

Seketoulie Keretsu[1]*, Pavithra K. Balasubramanian[1]*, Swapnil P. Bhujbal[1], and Seung Joo Cho[1,2]†

Abstract

Vascular endothelial growth factor (VEGF) is an important signaling protein involved in angiogenesis, which is the formation of new blood vessels from pre-existing vessels. Consequently, blocking of the vascular endothelial growth factor receptor (VEGFR-2) by small molecule inhibitors leads to the inhibition of cancer induced angiogenesis. In this study, we performed a two dimensional quantitative structure activity relationship (2D-QSAR) study of 38 N-Phenyl-N'-{4-(4-quinolyloxy) phenyl} urea derivatives as VEGFR-2 inhibitors based on hologram quantitative structure−activity (HQSAR). The model developed showed reasonable q^2=0.521 and r^2=0.932 values indicating good predictive ability and reliability. The atomic contribution map analysis of most active compound (compound **7**) indicates that hydrogen and oxygen atoms in the side chain of ring A and oxygen atom in side chain of ring C contributes positively to the activity of the compounds. The HQSAR model developed and the atomic contribution map can serve as a guideline in designing new compounds for VEGFR-2 inhibition.

Keywords: VEGF Kinase, VEGFR-2, HQSAR, Angiogenesis

1. Introduction

Angiogenesis is the formation of new blood vessels from pre-existing vessels[1]. This process involves the migration, growth, and differentiation of endothelial cells, which line the inside wall of blood vessels. Over-expression of several angiogenic factors has been observed in a variety of human tumors. Recently, it has been reported that the specific inhibition of tumor-induced angiogenesis suppresses the growth of many types of solid tumors[2,3].

Vascular endothelial growth factor (VEGF) is an important signaling protein involved in both vasculogenesis and angiogenesis and is secreted by malignant tumors[4]. The involvement of VEGF in tumor neoangiogenesis was first indicated by observations that many tumor cell lines produce VEGF and by the abundance of VEGF in tumors[5]. Of the known VEGF receptors such as (VEGFR-1, VEGFR-2 and VEGFR-3), the vascular endothelial growth factor receptor (VEGFR-2) is known to mediate almost all of the known cellular responses to VEGF[6]. The blockage of VEGFR-2 signaling by small molecule inhibitors to the VEGFR-2 kinase domain has been shown to inhibit angiogenesis, tumor progression, and dissemination in a number of preclinical and clinical studies. Hence, research relating to the inhibition of VEGFR-2 has emerged as an interesting topic for therapeutic drug design targeting cancer.

A number of small compounds that inhibits the activity of VEGF has already been produced such as, the 3-substituted indolinones, i.e., SU5416[7,8] and SU6668[9] the 4-anilinoquinazolines, such as ZD4190[9] and ZD6474[10] and the anilinophthalazines, such as CGP79787/PTK787[11]. The inhibitors work by interfering with various steps in angiogenesis by either recognizing and binding to the VEGF or by binding to the VEGF receptor on the surface of the endothelia cell or other proteins in the

[1]Department of Biomedical Sciences, College of Medicine, Chosun University, Gwangju 501-759, Republic of Korea
[2]Department of Cellular·Molecular Medicine, College of Medicine, Chosun University, Gwangju 501-759, Republic of Korea

*Authors have contributed equally to this work
†Corresponding author : chosj@chosun.ac.kr
(Received : August 22, 2017, Revised : September 15, 2017, Accepted : September 25, 2017)

downstream signaling pathways. Several small molecule inhibitors of VEGFR-2, such as Imatinib, Gefitinib, Erlotinib, Sunitinib, Sorafenib, and Dasatinib, have been approved very effective for the treatment of cancers[12]. In addition, bevacizumab, Sunitinib and Sorafenib have been approved by the Food and Drug Association (FDA) for treatment of cancer[13]. Recently, a novel series of VEGFR-2 inhibitors which can selectively inhibit VEGFR-2 with high inhibitory activities has been reported[14]. However, as the VEGF pathway is not only essential for normal growth and development, but also critical to physiological response and homeostasis in many organs and functions in adulthood, a variety of adverse effects were observed in clinical experiment resulting from the blockage of this pathway. The adverse effects attributed to VEGF inhibition include hypertension, arterial thromboembolic events (ATEs), proteinuria or renal dysfunction, wound complications, hemorrhage, gastrointestinal perforation, and reversible posterior leukoencephalopathy syndrome[15,16]. However, the molecular mechanisms of the adverse effects resulting due to the inhibition of VEGFR-2 are not fully understood[15]. Hence, further study to understand the mechanism of interaction between the small compounds and VEGFR-2 receptor and the effect on its activity is crucial.

Over the last few decades, with increase in computational power, quantitative structure activity relationship (QSAR) studies that relate structure of compounds to its biological activities has emerged as a popular technique in drug discovery[17,18]. Several QSAR and 3D-QSAR studies to find structure activity relation of VEGFR-2 inhibitors have already been reported[19-21]. Recently, Ugale et al,. performed 3D-QSAR studies of quinolone derivatives as VEGFR-2 tyrosine kinase inhibitors.[14] In this study, we used hologram quantitative structure–activity relationships (HQSAR) technique to study the structure-activity relation of a series of N-Phenyl-N'-{4-(4-quinolyloxy)phenyl} urea derivatives[22] as VEGFR-2 inhibitors with the objective to provide further insight into the key structural features required to design potential drug candidates.

2. Methodology

2.1. Dataset

We have performed HQSAR study on a series of 38 N-Phenyl-N'-{4-(4-quinolyloxy)phenyl} urea derivatives (shown in Table 1), which were reported in previous study as potent VEGFR-2 tyrosine kinase inhibitors[22]. For HQSAR study, the compounds were sketched and optimized by energy minimization with tripos force field using SYBYL-X 2.1[23] and Gasteiger-Hückel charges were applied as partial charges. Since the biological activity values are given in IC_{50} values, we also converted the IC_{50} values to pIC_{50} values for the HQSAR study.

2.2. HQSAR Technique

Hologram quantitative structure–activity relationships (HQSAR) is a 2D-QSAR protocol (Tripos Associates, Inc.) and it eliminates the need for determination of 3D structure, putative binding conformations and molecular alignment. In HQSAR, each molecule in the database is broken down into a series of unique structural fragments, which are arranged to form a molecular hologram[24]. The HQSAR program highlights substructural features in sets of molecules that are relevant to biological activity. HQSAR model development uses 2D structure directed fragment fingerprint. Based on the hologram length (HL) parameter given, these molecular fingerprints are broken into strings at fixed intervals. The HL determines the number of bins in the hologram into which the fragments are hashed. The optimal HQSAR model was derived from screening through the 12 default HL values, which were a set of 12 prime numbers ranging from 53-401. The model development was performed using the following parameters: atom (A), bond (B), connection (C), chirality (Ch), hydrogen (H) and donor/acceptor (DA). The validity of the model depends on statistical parameters such as cross validation q^2 and r^2 by Leave-Out-One (LOO) validation method[25].

3. Results and Discussion:

In the HQSAR analysis, we tried the different combinations of fraction distinctions namely, atom (A), bond (B), connection (C), chirality (Ch), hydrogen (H) and donor/acceptor (DA), to investigate the influence of fraction distinctions on the key statistical parameters such as q^2 and r^2. Following this, based on the combination of fraction distinction that gave the best statistical result, we also investigated the influence of fragment size on the results[26].

The combination A, B, C, Ch gave the best statistical

Table 1. Structure and pIC_{50} values of the 6-substituted 2-arylaminopurines derivatives

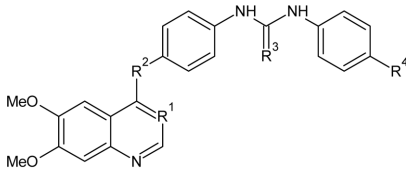

A

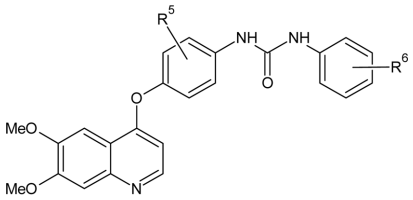

B

Compound	Structure	R^1	R^2	R^3	R^4	R^5	R^6	IC_{50}
Cpd01	A	CH	O	O	OMe	-	-	8.959
Cpd02	A	N	O	O	OMe	-	-	8.658
Cpd03	A	CH	S	O	OMe	-	-	8.229
Cpd04	A	CH	O	O	F	-	-	9.398
Cpd05	A	CH	O	S	F	-	-	7.000
Cpd06	B	-	-	-	-	H	H	9.699
Cpd07	B	-	-	-	-	H	2-OMe	9.699
Cpd08	B	-	-	-	-	H	4-OMe	8.959
Cpd09	B	-	-	-	-	H	2-Me	8.638
Cpd10	B	-	-	-	-	H	3-Me	9.699
Cpd11	B	-	-	-	-	H	4-Me	9.301
Cpd12	B	-	-	-	-	H	2-NO_2	7.721
Cpd13	B	-	-	-	-	H	3-NO_2	8.959
Cpd14	B	-	-	-	-	H	4-NO_2	8.252
Cpd15	B	-	-	-	-	H	2-F	9.301
Cpd16	B	-	-	-	-	H	3-F	8.921
Cpd17	B	-	-	-	-	H	4-F	9.398
Cpd18	B	-	-	-	-	H	3-Cl	8.796
Cpd19	B	-	-	-	-	H	4-Cl	9.699
Cpd20	B	-	-	-	-	H	2,3-F_2	9.155
Cpd21	B	-	-	-	-	H	2,4-F_2	9.155
Cpd22	B	-	-	-	-	H	2,5-F_2	9.398
Cpd23	B	-	-	-	-	H	2,6-F_2	8.745
Cpd24	B	-	-	-	-	H	3,4-F_2	8.959
Cpd25	B	-	-	-	-	H	3,5-F_2	8.745
Cpd26	B	-	-	-	-	H	2,3-Cl_2	7.569
Cpd27	B	-	-	-	-	H	2,4-Cl_2	8.252
Cpd28	B	-	-	-	-	H	2,5-Cl_2	8.222
Cpd29	B	-	-	-	-	H	2,6-Cl_2	7.432
Cpd30	B	-	-	-	-	H	3,4-Cl_2	8.432
Cpd31	B	-	-	-	-	H	3,5-Cl_2	8.051
Cpd32	B	-	-	-	-	2-F	2,4-F_2	9.046
Cpd33	B	-	-	-	-	2-Cl	2,4-F_2	9.398
Cpd34	B	-	-	-	-	3-Cl	2,4-F_2	8.585
Cpd35	A	CH	NH	O	OMe	-	-	7.000
Cpd36	A	CH	O	NCN	F	-	-	7.260
Cpd37	B	-	-	-	-	H	3-OMe	9.000
Cpd38	B	-	-	-	-	2-F	2,4-F_2	9.000

Table 2. HQSAR models with different statistical parameters

Model	Fragment distinction	q^2	r^2	SDEP	SEE	NOC	BHL
1.	A/B	0.526	0.832	0.546	0.325	4	151
2.	A/C	0.478	0.837	0.573	0.32	4	257
3.	B/C	0.392	0.664	0.609	0.453	3	97
4.	A/B/C	0.467	0.819	0.70	0.333	3	257
5.	A/B/Ch	0.518	0.897	0.559	0.259	5	199
6.	C/H/Ch	0.021	0.204	0.751	0.678	1	151
7.	A/C/DA	0.325	0.620	0.692	0.482	3	97
8.	A/B/C/Ch	0.431	0.823	0.590	0.329	3	257
9.	A/B/H/DA	0.158	0.511	0.707	0.538	2	307
10.	A/B/C/Ch/DA	0.301	0.601	0.653	0.494	3	199
11.	**A/B/C/H/Ch**	**0.521**	**0.932**	**0.566**	**0.213**	**6**	**150**
12.	A/B/C/H/DA	0.325	0.620	0.642	0.482	3	97
13.	A/B/C/H/DA/Ch	0.200	0.547	0.699	0.526	3	199

Note: Here, A= atom, B=bond, C=connection, H=hydrogen, Ch=chirality, DA=hydrogen bond donor/acceptor, NOC=number of components, q^2=cross-validated correlation coefficient, SDEP=cross-validated standard error of prediction, r^2=non-cross-validated correlation coefficient, SEE=standard error of estimate, BHL=best hologram length. Model selected to exploit atom count parameter is shown in bold face.

Table 3. Statistical summary of A/B/C/Ch model explored for the different atom counts. Final model selected for HQSAR analysis is represented in bold

Atom Count	q^2	r^2	SDEP	SEE	NOC	BHL
1-4	0.358	0.767	0.646	0.389	5	353
2-5	0.355	0.834	0.658	0.333	6	151
3-6	0.466	0.899	0.598	0.272	6	151
4-7	**0.521**	**0.932**	**0.566**	**0.213**	**6**	**151**
5-8	0.385	0.822	0.613	0.329	3	199
6-9	0.391	0.898	0.169	0.253	4	199
7-10	0.452	0.932	0.596	0.210	5	257
8-11	0.487	0.949	0.586	0.184	6	151

results and hence further analysis for different fragment size was done based on this combination. The statistical results of the different combination of fraction distinctions are shown in Table 2. The cross validated PLS analysis gave a q^2 value of 0.521 and r^2 value of 0.932 with 6 optimal number of components (ONC) and standard error of estimation (SEE) value of 0.213. It is also observed that the default fragment size (4-7) gave the best statistical result. The actual and predicted activity values for the selected model are given in Table 4. The scatter plot for the same is shown in Fig. 1.

We also analyzed the atomic contribution of the most active compound (compound **7**) and the least active compound (compound **35**) which are shown in Fig. 2(a) and Fig. 2(b) respectively. The dataset molecules had a common substructure and varied at in A, B, C and D substructure. In the atom contribution map shown in Fig. 2, a yellow, green-blue and green indicated favorable or positive contribution to the activity, while unfavorable and negative contribution to the activity was denoted by red, red-orange and orange[26,27].

As observed from the contribution map of the most active compound (compound **7**) shown in Fig. 2(a), the oxygen, hydrogen and carbon atoms from the side chain of ring A contributed favorably to the activity (pIC_{50}= 9.699). Also the green color at the oxygen atom between

Table 4. Actual pIC_{50} and predicted pIC_{50} with their residual values of selected HQSAR model.

Compound	Actual pIC_{50}	HQSAR	
		Predicted	Residual
Cpd01	8.959	9.075	-0.116
Cpd02	8.658	8.717	-0.059
Cpd03	8.229	8.191	0.038
Cpd04	9.398	9.413	-0.015
Cpd05	7.000	7.047	-0.047
Cpd06	9.699	9.545	0.154
Cpd07	9.699	9.122	0.577
Cpd08	8.959	9.075	-0.116
Cpd09	8.638	8.838	-0.200
Cpd10	9.699	9.468	0.231
Cpd11	9.301	9.459	-0.158
Cpd12	7.721	8.104	-0.383
Cpd13	8.959	8.651	0.308
Cpd14	8.252	8.651	-0.399
Cpd15	9.301	9.198	0.103
Cpd16	8.921	9.168	-0.247
Cpd17	9.398	9.413	-0.015
Cpd18	8.796	8.870	-0.074
Cpd19	9.699	9.154	0.545
Cpd20	9.155	8.808	0.347
Cpd21	9.155	9.304	-0.149
Cpd22	9.398	9.129	0.269
Cpd23	8.745	9.066	-0.321
Cpd24	8.959	9.023	-0.064
Cpd25	8.745	9.049	-0.304
Cpd26	7.569	8.107	-0.538
Cpd27	8.252	8.320	-0.068
Cpd28	8.222	8.345	-0.123
Cpd29	7.432	7.856	-0.424
Cpd30	8.432	8.596	-0.164
Cpd31	8.051	8.222	-0.171
Cpd32	9.046	8.965	0.081
Cpd33	9.398	8.412	0.986
Cpd34	8.585	8.591	-0.006
Cpd35	7.000	6.895	0.105
Cpd36	7.260	6.770	0.490
Cpd37	9.000	9.074	-0.074
Cpd38	9.000	8.990	0.010

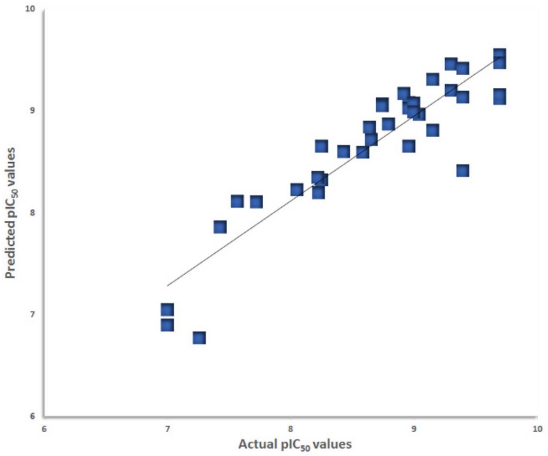

Fig. 1. Scatter plot diagram for HQSAR analysis. Plot shows the actual and predicted pIC50 values of compounds.

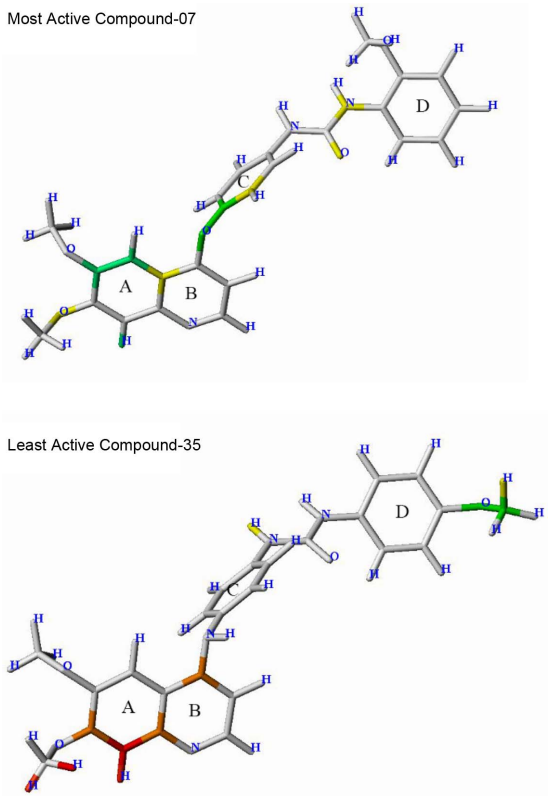

Fig. 2. HQSAR atomic contribution maps. (a) Most active compound-07 (b) Least active compound-35.

ring B and C indicated that the oxygen atom contribute positively to the activity. Also, the yellow color coded oxygen and nitrogen atoms between ring C and ring D indicate that these atoms contribute positively to the

activity of the compound. Over all, there was no red, red-orange or orange color coded atom in the most active compound. In contrast to this, the least active compound (compound **35**) shown in Fig. 2(b) has hydrogen atoms in the side chain of ring A and also nitrogen and carbon atoms color coded in red indicating negative contribution to the activity (pIC_{50}= 7.0). Similar results were also observed in the atomic contribution map of compound 5 (pIC_{50}= 7.0) where, the hydrogen and carbon in the side chains of ring A and B were coded in red and orange color indicating negative contribution to the activity.

4. Conclusion

The developed HQSAR model was based on the fraction distinction combination of atom (A) and bond (B) connection (C), chirality (Ch) and default fragment size. The cross validated PLS analysis gave a q^2 value of 0.521 and r^2 value of 0.932 indicating that the developed model has acceptable predictive ability and reliability. The atomic contribution map analysis suggests that the oxygen, hydrogen and carbon in the side chain of ring A and the oxygen atom at the side chain of ring C contributes positively to the activity of compounds, whereas nitrogen atom in side chain of ring B contributes negatively to the activity of compounds. The HQSAR model developed reveals the contribution and importance of atoms and functional groups on the activity of the dataset compounds. This study may serve as a guideline in designing novel active compounds for VEGFR-2 inhibition.

Acknowledgements

This work was supported by the National Research Foundation of Korea Grant funded by the Korean Government (NRF-2016R1D1A1B01007060).

References

[1] J. Folkman, “Anti-angiogenesis: new concept for therapy of solid tumors”, Ann. Surg., Vol. 175, pp. 409-416, 1972.

[2] G. Bergers, K. Javaherian, K.-M. Lo, J. Folkman, and D. Hanahan, “Effects of angiogenesis inhibitors on multistage carcinogenesis in mice”, Science, Vol. 284, pp. 808-812, 1999.

[3] T.-P. D. Fan, R. Jagger, and R. Bicknell, “Controlling the vasculature: angiogenesis, anti-angiogenesis and vascular targeting of gene therapy”, Trends Pharmacol. Sci., Vol. 16, pp. 57-66, 1995.

[4] K. J. Kim, B. Li, J. Winer, M. Armanini, N. Gillett, H. S. Phillips, and N. Ferrara, “Inhibition of vascular endothelial growth factor-induced angiogenesis suppresses tumour growth in vivo”, Nature, Vol. 362, pp. 841-844, 1993.

[5] W. Kolch, G. Martiny-Baron, A. Kieser, and D. Marmé, “Regulation of the expression of the VEGF/VPS and its receptors: role in tumor angiogenesis”, Breast Cancer Res. Treat., Vol. 36, pp. 139-155, 1995.

[6] W. P. Leenders, “Targetting VEGF in anti-angiogenic and anti-tumour therapy: Where are we now?”, Int. J. Exp. Pathol., Vol. 79, pp. 339-346, 1998.

[7] T. A. T. Fong, L. K. Shawver, L. Sun, C. Tang, H. App, T. J. Powell, Y. H. Kim, R. Schreck, X. Wang, W. Risau, A. Ullrich, K. P. Hirth, and G. McMahon, “SU5416 is a potent and selective inhibitor of the vascular endothelial growth factor receptor (Flk-1/KDR) that inhibits tyrosine kinase catalysis, tumor vascularization, and growth of multiple tumor types”, Cancer res, Vol. 59, pp. 99-106, 1999.

[8] L. Sun, N. Tran, F. Tang, H. App, P. Hirth, G. McMahon, and C. Tang, “Synthesis and biological evaluations of 3-substituted indolin-2-ones: a novel class of tyrosine kinase inhibitors that exhibit selectivity toward particular receptor tyrosine kinases”, J. Med. Chem., Vol. 41, pp. 2588-2603, 1998.

[9] L. Sun, N. Tran, C. Liang, F. Tang, A. Rice, R. Schreck, K. Waltz, L. K. Shawver, G. McMahon, and C. Tang, “Design, synthesis, and evaluations of substituted 3-[(3-or 4-carboxyethylpyrrol-2-yl) methylidenyl] indolin-2-ones as inhibitors of VEGF, FGF, and PDGF receptor tyrosine kinases”, J. Med. Chem., Vol. 42, pp. 5120-5130, 1999.

[10] L. F. Hennequin, E. S. Stokes, A. P. Thomas, C. Johnstone, P. A. Plé, D. J. Ogilvie, M. Dukes, S. R. Wedge, J. Kendrew, and J. O. Curwen, “Novel 4-anilinoquinazolines with C-7 basic side chains: design and structure activity relationship of a series of potent, orally active, VEGF receptor tyrosine kinase inhibitors”, J. Med. Chem., Vol. 45, pp. 1300-1312, 2002.

[11] G. Bold, K.-H. Altmann, J. Frei, M. Lang, P. W. Manley, P. Traxler, B. Wietfeld, J. Brüggen, E. Buchdunger, R. Cozens, S. Ferrari, P. Furet, F. Hofmann, G. Martiny-Baron, J. Mestan, J. Rösel, M. Sills, D. Stover, F. Acemoglu, E. Boss, R.

Emmenegger, L. Lässer, E. Masso, R. Roth, C. Schlachter, W. Vetterli, D. Wyss, and J. M. Wood, "New anilinophthalazines as potent and orally well absorbed inhibitors of the VEGF receptor tyrosine kinases useful as antagonists of tumor-driven angiogenesis", J. Med. Chem., Vol. 43, pp. 2310-2323, 2000.

[12] N. A. G. Lankheet, M. J. X. Hillebrand, H. Rosing, J. H. Schellens, J. H. Beijnen, and A. D. R. Huitema, "Method development and validation for the quantification of dasatinib, erlotinib, gefitinib, imatinib, lapatinib, nilotinib, sorafenib and sunitinib in human plasma by liquid chromatography coupled with tandem mass spectrometry", Biomed. Chromatogr., Vol. 27, pp. 466-476, 2013.

[13] T. K. Choueiri, F. A. Schutz, Y. Je, J. E. Rosenberg, and J. Bellmunt, "Risk of arterial thromboembolic events with sunitinib and sorafenib: a systematic review and meta-analysis of clinical trials", J. Clin. Oncol., Vol. 28, pp. 2280-2285, 2010.

[14] V. G. Ugale, H. M. Patel, and S. J. Surana, "Molecular modeling studies of quinoline derivatives as VEGFR-2 tyrosine kinase inhibitors using pharmacophore based 3D QSAR and docking approach", Arabian Journal of Chemistry, Vol. 10, pp. S1980-S2003, 2017.

[15] H. X. Chen and J. N. Cleck, "Adverse effects of anticancer agents that target the VEGF pathway", Nat. Rev. Clin. Oncology., Vol. 6, pp. 465-477, 2009.

[16] T. Kamba and D. M. McDonald, "Mechanisms of adverse effects of anti-VEGF therapy for cancer", Br. J. cancer, Vol. 96, pp. 1788-1795, 2007.

[17] J. Verma, V. M. Khedkar, and E. C. Coutinho, "3D-QSAR in drug design-a review", Curr. Top. Med. Chem, Vol. 10, pp. 95-115, 2010.

[18] A. Z. Dudek, T. Arodz, and J. Gálvez, "Computational methods in developing quantitative structure-activity relationships (QSAR): a review", Comb. Chem. high throughput screen., Vol. 9, pp. 213-228, 2006.

[19] H. Zeng and H. Zhang, "Combined 3D-QSAR modeling and molecular docking study on 1, 4-dihydroindeno [1, 2-c] pyrazoles as VEGFR-2 kinase inhibitors", J. Mol. Graph. Model., Vol. 29, pp. 54-71, 2010.

[20] M. M. Neaz, F. A. Pasha, M. Muddassar, S. H. Lee, T. Sim, J.-M. Hah, and S. J. Cho, "Pharmacophore based 3D-QSAR study of VEGFR-2 inhibitors", Med. Chem. Res., Vol. 18, pp. 127-142, 2009.

[21] C. Muñoz, F. Adasme, J. H. Alzate-Morales, A. Vergara-Jaque, T. Kniess, and J. Caballero, "Study of differences in the VEGFR2 inhibitory activities between semaxanib and SU5205 using 3D-QSAR, docking, and molecular dynamics simulations", J. Mol. Graph. Model., Vol. 32, pp. 39-48, 2012.

[22] K. Kubo, T. Shimizu, S.-I. Ohyama, H. Murooka, A. Iwai, K. Nakamura, K. Hasegawa, Y. Kobayashi, N. Takahashi, K. Takahashi, S. Kato, T. Izawa, and T. Isoe, "Novel potent orally active selective VEGFR-2 tyrosine kinase inhibitors: synthesis, structure−activity relationships, and antitumor activities of n-phenyl-n '-{4-(4-quinolyloxy) phenyl} ureas", J. Med. Chem., Vol. 48, pp. 1359-1366, 2005.

[23] M. Clark, R. D. Cramer, and N. Van Opdenbosch, "Validation of the general purpose Tripos 5.2 force field", J. Comput. Chem., Vol. 10, pp. 982-1012, 1989.

[24] M. A. Avery, M. Alvim-Gaston, C. R. Rodrigues, E. J. Barreiro, F. E. Cohen, Y. A. Sabnis, and J. R. Woolfrey, "Structure−activity relationships of the antimalarial agent artemisinin. 6. The development of predictive in vitro potency models using CoMFA and HQSAR methodologies", J. Med. Chem., Vol. 45, pp. 292-303, 2002.

[25] C. R. Rodrigues, T. M. Flaherty, C. Springer, J. H. McKerrow, and F. E. Cohen, "CoMFA and HQSAR of acylhydrazide cruzain inhibitors", Bioorg. Med. Chem. Lett., Vol. 12, pp. 1537-1541, 2002.

[26] W. Zhu, G. Chen, L. Hu, X. Luo, C. Gui, C. Luo, C. M. Puah, K. Chen, and H. Jiang, "QSAR analyses on ginkgolides and their analogues using CoMFA, CoMSIA, and HQSAR", Bioorg. Med. Chem., Vol. 13, pp. 313-322, 2005.

[27] S. P. Bhujbal, S. Keretsu, and S. J. Cho, "HQSAR study on substituted 1H-pyrazolo [3, 4-b] pyridines derivatives as FGFR kinase antagonists", J. Chosun Natural Sci., Vol. 10, pp. 85-94, 2017.